Super resolution imaging of nanoparticles cellular uptake and trafficking

Super Resolution Imaging of Nanoparticles Cellular Uptake and Trafficking

Daan van der Zwaag[1,2†], Nane Vanparijs[3†], Sjors Wijnands[1,4], Riet De Rycke[5], Bruno G. De Geest[2*] and Lorenzo Albertazzi[1,6*]

[1]*Institute for Complex Molecular Systems, Eindhoven University of Technology, Eindhoven, Netherlands*
[2]*Department of Chemical Engineering and Chemistry, Eindhoven University of Technology, Eindhoven, The Netherlands*
[3]*Department of Pharmaceutics, Ghent University, Ghent, Belgium*
[4]*Department of Biomedical Engineering, Eindhoven University of Technology, Eindhoven, The Netherlands*
[5]*VIB Department for Molecular Biomedical Research, Technologiepark 927, 9052 Ghent, Belgium*
[6]*Institute for Bioengineering of Catalonia (IBEC), Barcelona, Spain*

† these authors equally contributed as first authors

** Prof. Dr. Bruno De Geest*
Department of Pharmaceutics, Ghent University, Ghent Belgium
br.degeest@ugent.be

** Dr. Lorenzo Albertazzi*
Institute for Bioengineering of Catalonia (IBEC), Barcelona, Spain
lalbertazzi@ibecbarcelona.eu

KEYWORDS: Nanoparticles, Delivery, Super Resolution Imaging, Cellular Uptake, STORM

ABSTRACT

Understanding the interaction between synthetic nanostructures and living cells is of crucial importance for the development of nanotechnology-based intracellular delivery systems. Fluorescence microscopy is one of the most widespread tools owing to its ability to image multiple colors in native conditions. However, due to the limited resolution, it is unsuitable to address individual diffraction-limited objects. Here we introduce a combination of super-resolution microscopy and single-molecule data analysis to unveil the behavior of nanoparticles during their entry into mammalian cells. Two-color Stochastic Optical Reconstruction Microscopy (STORM) addresses the size and positioning of nanoparticles inside cells and probes their interaction with the cellular machineries at nanoscale resolution. Moreover, we develop image analysis tools to extract quantitative information about internalized particles from STORM images. To demonstrate the potential of our methodology, we extract previously inaccessible information by the direct visualization of the nanoparticle uptake mechanism and the intracellular tracking of nanoparticulate model antigens by dendritic cells. Finally, a direct comparison between STORM, confocal microscopy and electron microscopy is presented, showing that STORM can provide novel and complementary information on nanoparticle cellular uptake.

Introduction

The use of nanoparticles for intracellular delivery of therapeutic molecules is a key application of nanotechnology and material chemistry[1]. In this framework, a variety of materials have been fabricated and evaluated *in vitro* and *in vivo.* [2]. However, the development of these complex materials is still challenging and a large majority of the investigated nanomedicines fails to be translated to the clinic[3]. A crucial factor limiting the rational design of effective nanomedicines is the inadequate understanding of nanoparticle-cell interactions[4]. Therefore, it is imperative to

acquire more detailed knowledge about the role of size, morphology, and surface chemistry in determining the cell binding, uptake and intracellular fate of nanoparticles[5]. Interactions between nanoparticles and cells are typically visualized using confocal laser scanning microscopy (CLSM) or electron microscopy (EM). Confocal microscopy allows for 3D multicolor imaging in live cells but is restricted to diffraction-limited resolution (≈ 250 nm), preventing the observation of individual nanoparticles. To bypass this limitation, innovative methodologies based on confocal spot intensity have been proposed; this has greatly helped the quantification of nanoparticle uptake but still cannot directly image and resolve individual nanoparticles inside cells[5]. On the contrary, electron microscopy offers an excellent resolution that allows examination of nanoparticles and subcellular structures with high detail, but only in fixed cells and at the cost of cumbersome sample preparation. Moreover, multicolor imaging and data interpretation are not always straightforward, especially in the case of soft materials that provide poor contrast[6]. Therefore, novel methods able to overcome these limitations are needed. Recently, super resolution microscopy has been proposed as a novel tool combining the advantages of optical microscopy with sub 50 nm resolution, thus representing an ideal bridge between confocal and electron microscopy[7]. A variety of super resolution techniques such as stimulated emission depletion (STED)[8], stochastic optical reconstruction microscopy (STORM)[9], photoactivation localization microscopy (PALM)[10] and structured illumination microscopy (SIM)[11] are successfully used in biological sciences to image cellular structures with sub-diffraction resolution. Recently the potential of super resolution microscopy has also been exploited in materials science and nanotechnology for the imaging of polymers[12], self-assembled materials[13] and DNA origami[14]. However, to date the use of super resolution techniques to probe material-cell interactions is rather unexplored, in particular in the field of nanomedicine.

Here we investigate cell binding, uptake and intracellular trafficking of nanoparticles using a combination of STORM microscopy and quantitative image analysis. STORM is based on the accurate localization of individual, stochastically blinking fluorophores and can provide high resolution images (≈ 20 nm)[9]. Although other super resolution techniques such as STED and SIM presents several interesting features for nanomaterials imaging such as a better temporal resolution, we chose STORM for its unique resolution as well as for the ability to achieve information at the single molecule level, e.g. molecule counting[15]. This potential is fostered by the image analysis methodology that yields information on nanoparticles at the single molecule level. Here, we propose a STORM-based methodology able to resolve sub-diffraction nanoparticles, probe their interactions with cellular structures by colocalization and extract quantitative information about the size, number and positioning of the internalized nanoparticles. Our method is validated by comparison with confocal microscopy and electron microscopy and we demonstrate its potential to obtain novel information on the uptake of nanoparticulate model-antigens by dendritic cells.

Results and discussion

Figure 1A schematically depicts the key steps in our methodology. In order to perform two-color imaging of nanomaterial interactions with cellular structures, we label nanoparticles and specific organelles with two spectrally separated, STORM-compatible dyes. Nanoparticles are labeled with either Cy5 or Alexa647, among the best performing STORM cyanine-based dyes[16], through EDC/NHS chemistry. We have evaluated the STORM suitability of several cellular stains that are commonly used in studies of drug delivery and have arrived at an array of labels to track the membrane binding and intracellular trafficking of nanoparticles. After nanoparticle administration, cells are fixed at a desired time point and imaged with nanometric

resolution using two-color direct STORM (dSTORM)[17]. The images are subsequently analyzed to obtain nanoparticle number, size and intracellular localization.

Figure 1B shows dSTORM imaging of 80 nm polystyrene (PS) nanoparticles internalized by HeLa cells. PS nanoparticles have been extensively evaluated as model nanomedicines, both for delivery and mechanistic purposes, due to their controlled size and ease of functionalization[18]. The plasma membrane of the HeLa was stained with Alexa568-labeled wheat germ agglutinin (WGA), a lectin known to bind to N-acetyl-D-glucosamine and sialic acid on the cell membrane[19]. This label allows us to freely choose the dye conjugated to the lectin and to easily control the density of labels on the membrane, both crucial factors for optimal STORM performance[16].

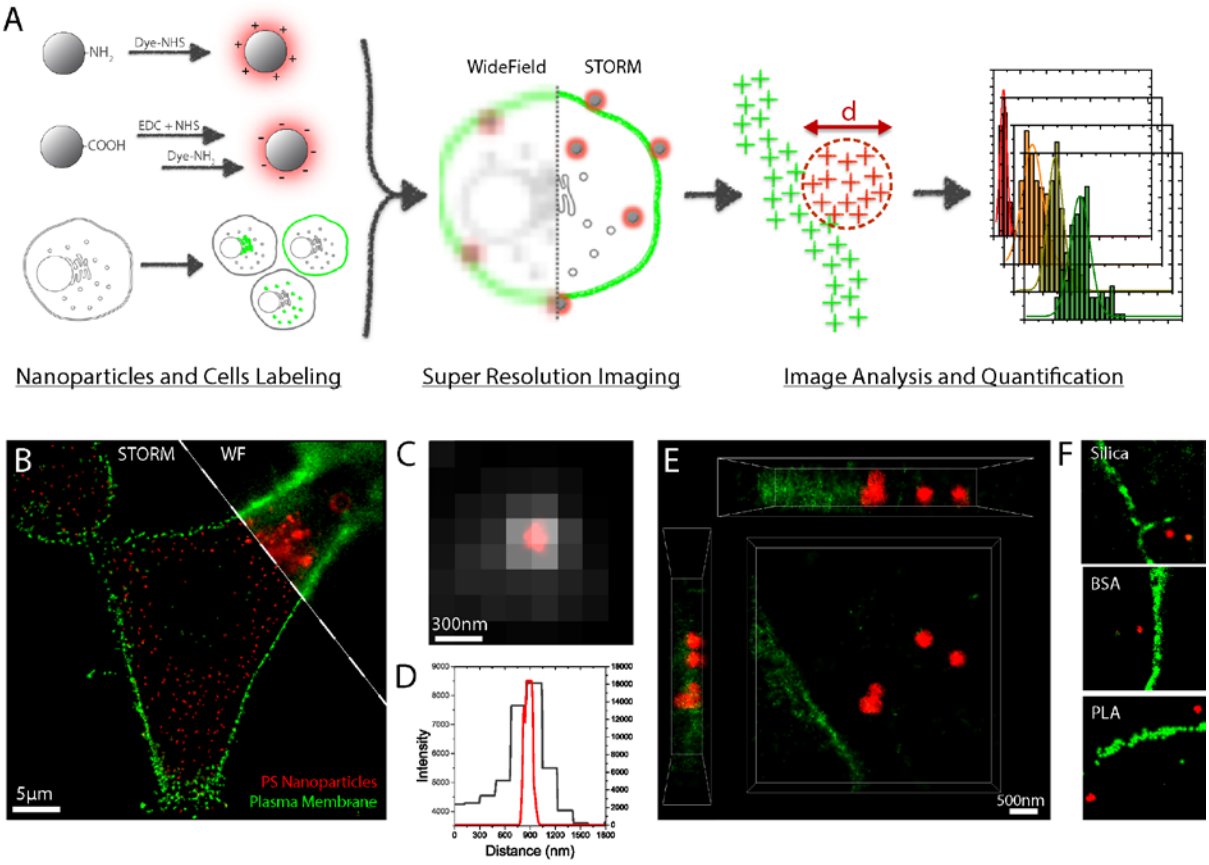

Figure 1 – STORM imaging of nanoparticle uptake by HeLa cells. A) Schematic representation of our methodology, comprising particle and cell labeling, STORM imaging and data analysis. B) STORM image of 80 nm PS nanoparticles inside membrane-stained HeLa cells (conventional wide-field image in the top right corner). C) Overlay of conventional wide-field image (gray) and STORM (red) of an individual nanoparticle. D) Profile of the nanoparticle in panel 1C for the STORM and conventional

wide-field image. E) 3D imaging of 330 nm NPs using astigmatism. F) Silica, crosslinked bovine serum albumin (BSA) and poly lactic acid (PLA) nanoparticles internalized by HeLa cells and imaged by STORM. Image size = 5 μm.

The comparison between STORM imaging and wide-field microscopy (top right corner) clearly shows the dramatic increase in resolution, allowing to resolve individual nanoparticles and their position inside the cell while the diffraction limited imaging is unable to resolve the details of the nanoparticle-membrane interactions. Figures 1C-D show the details of an individual nanoparticle in STORM (red) and conventional wide-field imaging (grey), highlighting the ability of STORM to resolve sub-diffraction limited nanoparticles (Figure 1D). As a further comparison, we imaged the same sample by confocal microscopy (See Figure S1). Despite the improvement of axial resolution and signal-to-noise ratio of confocal microscopy compared to wide-field microscopy, the particles still appear significantly larger due to the diffraction limit.

Resolving nanoparticles in three dimensions is of crucial importance for intracellular tracking. Here we use astigmatism-based STORM imaging[20] to resolve the 3D structure of internalized nanoparticles; Figure 1E shows top and sides views of 330 nm nanoparticles in WGA-stained HeLa cells. The z-resolution of STORM yields the correct size and shape of the polystyrene beads and their 3D positioning inside cells, as well as the local curvature of the membrane (See Figure S2). Nanometric sectioning (see Figure S3) allows the accurate assignment of clusters of nanoparticles, which appear otherwise superimposed in the 2D projection. The enhancement of resolution compared to conventional techniques is particularly striking in z-direction, as shown by the 3D confocal imaging of the same sample (Figure S4) in which the particles appears axially elongated. To prove the general applicability of our methodology, we have labeled a variety of relevant carriers used in nanomedicine, such as poly lactic acid (PLA) NPs, silica colloids and crosslinked bovine serum albumin (BSA) nanoparticles with suitable STORM dyes. These materials are widely used in nanomedicine research and are currently

being evaluated in clinical trials for the delivery of hydrophobic drugs, gene delivery, vaccines and cancer immunotherapy[21]. Figure 1F shows 2 color images of 250 nm particles of the different materials internalized by HeLa cells. STORM successfully resolves these sub-diffraction particles, showing that the performance of the technique is minimally affected by the chemical nature of the materials and proving that our approach can be applied to a wide variety of synthetic nanoparticles. To further demonstrate the power of our methodology, we studied of the mechanism of nanoparticle entry in HeLa cells. Typically, nanoparticles enter cells by endocytosis after membrane binding. Several internalization pathways are possible, including macropinocytosis, clathrin-mediated endocytosis and caveolin-mediated endocytosis[22]. The understanding of the entry pathway is of crucial importance towards applications in drug delivery as different endocytic routes imply different biochemical environments around the drug carrier. For example, macropinocytosis and clathrin-mediated endocytosis are known to traffic the nanoparticles to acidic compartments and this route can be exploited for pH-triggered drug release[23]. Co-localization with endocytosis markers is a widely used method to investigate internalization pathways but its accuracy is often limited by the resolution of the confocal microscope that does not allow to solve the sub-diffraction endocytic vesicles[24]. Here, in order to probe the interactions with intracellular organelles after internalization, we explored cellular labels[25] for super resolution colocalization to target organelles relevant in nanomedicine delivery. Figure 2A shows the co-localization of 80 nm PS nanoparticles with plasma membrane, macropinosome, nuclear membrane and actin markers (for an enlarged version please refer to Fig. S5). Notably, we decided not to use immunostaining, aiming to simplify our methodology and to avoid the resolution issues related to the size of the antibodies[26].

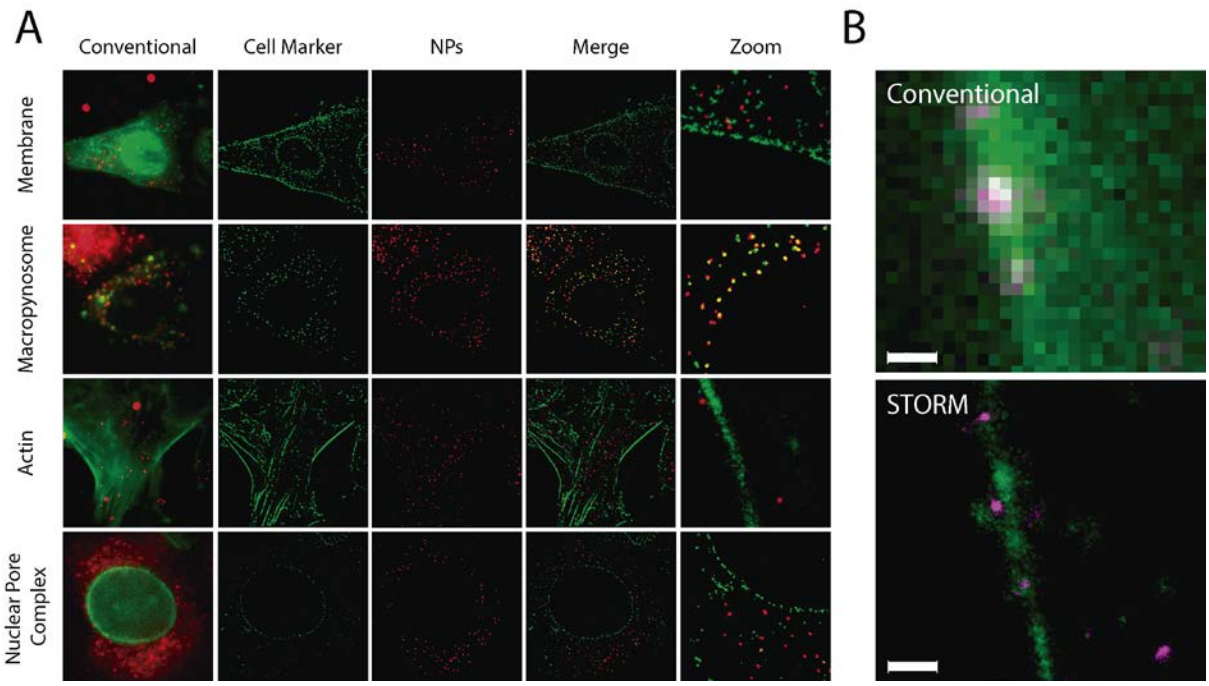

Figure 2 – A) Super resolution co-localization of organelle markers (green) and internalized 80 nm PS nanoparticles (red). Image size = 40 µm, zoomed image size = 5 µm. B) Super resolution images of a micropinocytosis event of a 220 nm PS nanoparticle (magenta). Plasma membrane is stained with WGA (green). Scale bar = 700 nm.

The ability to clearly resolve individual vesicles and nanoparticles makes the co-localization more accurate and the identification of the organelle involved in NP uptake straightforward. STORM analysis reveals strong co-localization of the particles with dextran-labeled endosomal vesicles, a marker for micropinocytosis. Based on these observations of endosomal pathways, we further investigated the initial stages of internalization. Figure 2B and Fig. S6 show the colocalization with WGA-labeled plasma membrane revealing membrane engulfing and macropinocytosis of individual nanoparticles, a molecular event so far only observed by TEM[27]. Notably, such a structure can be damaged during the fixation process. The success of the sample preparation strongly relies on the choice of the fixation procedure as well as on the surface chemistry of the nanoparticles (e.g. amine-functionalized particles are more strongly fixed). The direct observation of such interactions between nanoparticles and cellular structures

is a powerful addition to existing indirect measurement tools and opens the way to more detailed studies of membrane binding, the key step of targeted delivery.

The development of quantitative imaging, "from pretty pictures to hard numbers"[28], is of great importance in the field of nanoscopy. The single molecule nature of STORM represents a challenge for data analysis but together with the corresponding high resolution, provides great potential to extract useful information at the molecular level. In order to quantify the details of nanoparticle entry into HeLa cells we developed an image analysis method able to process two-color STORM images, as schematically shown in Figure 3 and extensively described in the Supporting Information. Our software separates the two channels and eliminates background localization through a density filter, i.e. only the dense localizations groups corresponding to nanoparticles are maintained while sparse points due to background noise are discarded. A clustering algorithm allows isolation of the separate groups of localizations that can now be investigated individually.

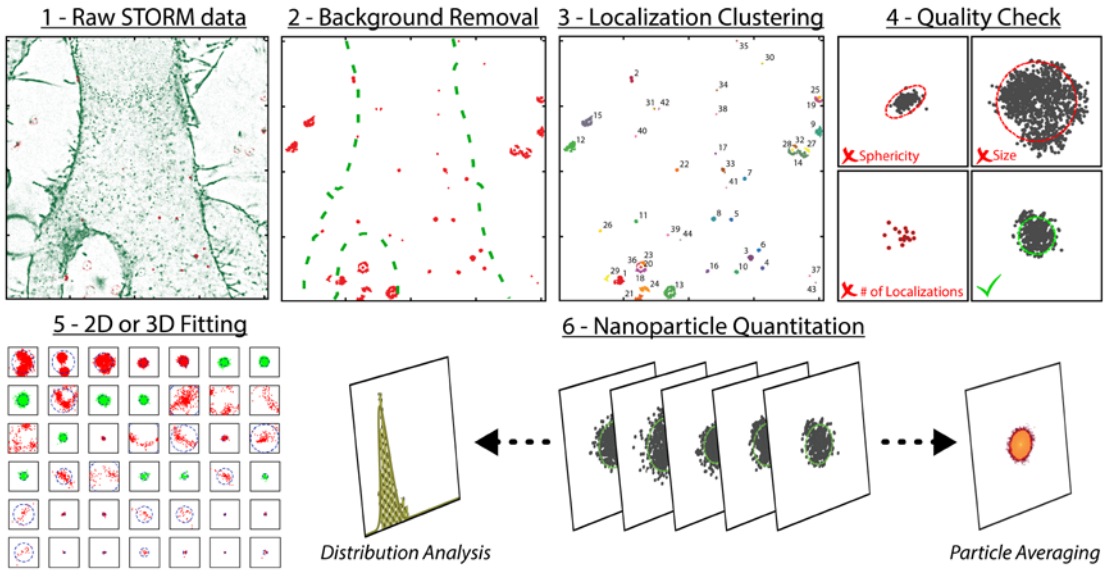

Figure 3 – Analysis routine for automated quantification of nanoparticle properties. In the six-step procedure illustrated here, individual nanoparticles are identified in large fields of view (steps 1-3) and, after a quality check (step 4), their properties are assessed with a fitting procedure (step 5). Based on the aggregated dataset, not only can the mean value of relevant characteristics be investigated, but also the corresponding variation (step 6). Additionally, spatial overlay of multiple nanoparticles, i.e. particle averaging, yields enhanced reconstruction and resolution.

Every cluster is subjected to a quality check that discards all signals not corresponding to individual nanoparticles. This is achieved through: i) a size filter that discards very small objects (likely single fluorescent molecules) and very big objects (likely aggregates of multiple nanoparticles); ii) a shape filter that eliminate high aspect ratio objects (e.g. dimers of nanoparticles) and iii) a number threshold that selects only the nanoparticles that provide a sufficient number of localizations and will result thus in accurate quantification. Notably, if necessary, the filter for nanoparticle size can be tuned to include intracellular NP clustering. Approved clusters are then fitted with a 2D (circles) or 3D (spheres) model that yields information about the size of the internalized NPs. This procedure allows for the automatic quantification of a large number of internalized nanoparticles, and subsequently the distribution of a specific property (e.g. size) can be plotted in a histogram or individual objects can be averaged to obtain a high resolution rendering of the nanoparticles. Particle averaging is a procedure commonly used in electron microscopy and was recently translated to optical nanoscopy[29]; in this procedure many individual objects are aligned on the basis of the fitting procedure and their localization is summed to obtain a high quality map of the nanoparticles that is representative of the full sample. In STORM, this has the particular advantage of allowing the selection of localizations with high brightness (and therefore accuracy) without losing the reconstruction of the object[30].

With this powerful tool at hand, we proceeded to quantify the cellular entry of a series of nanoparticles varying in size and chemical composition. Figure 4 shows the images of internalized nanoparticles with diameters ranging from 80 nm to 800 nm in wide-field (Figure 4A) and STORM (Figure 4B). Clearly, the nanoparticles above the diffraction limit (450 nm and 880 nm) can be resolved by both techniques, while below that limit only STORM is able to precisely address the size of individual nanoparticles. Moreover, the resolution of the plasma membrane is also enhanced in STORM, providing more information about NP-cell

interactions. From the analysis of multiple cells with the previously described method, a global picture of nanoparticle entry in HeLa cells can be obtained.

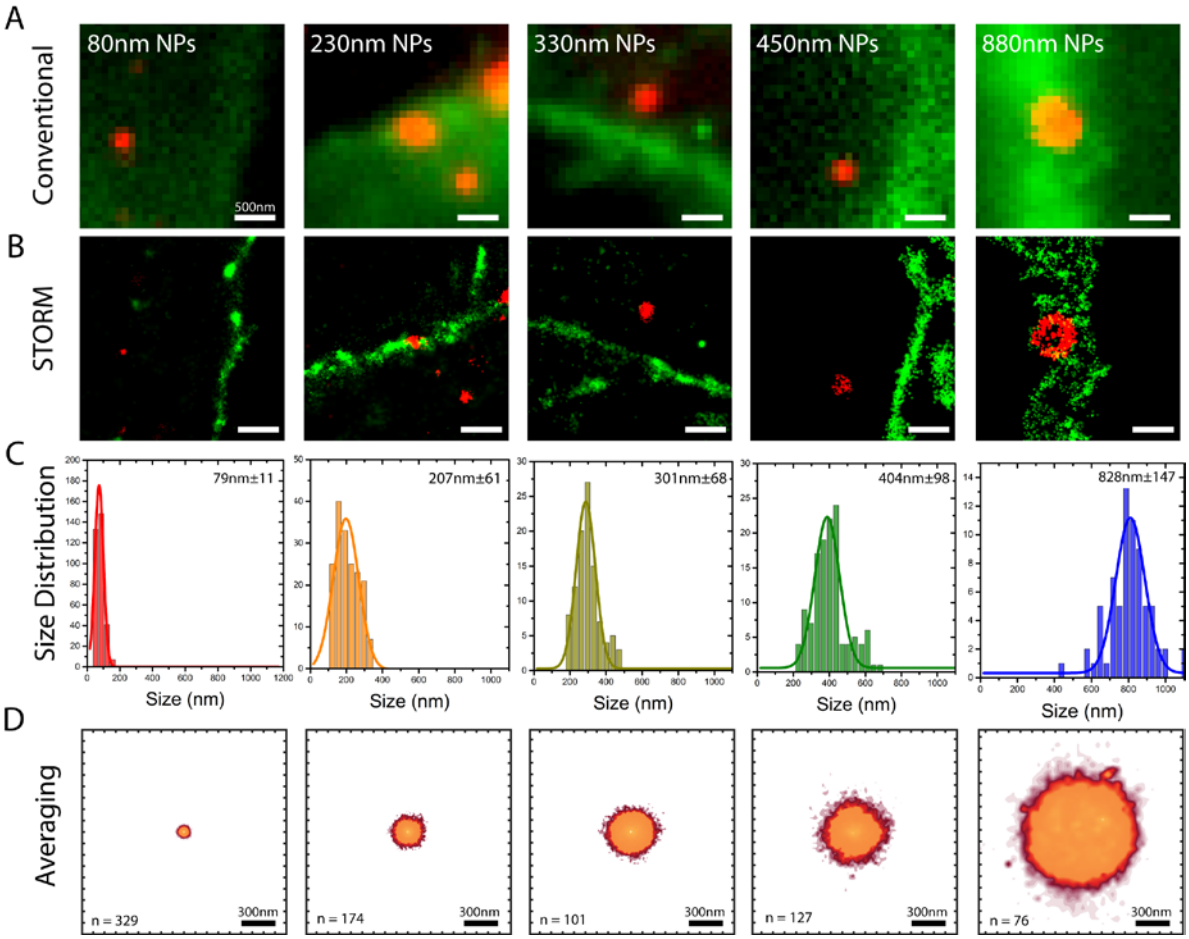

Figure 4 – Analysis of nanoparticles of different sizes internalized by HeLa cells. NPs are commercially available and have been further characterized by DLS. Cells were imaged with conventional wide-field (A) and STORM (B) microscopy. The automated image analysis identifies individual nanoparticles and provides a quantification of their properties through size histogram (C) particle averaging (D).

Figure 4C shows the histogram of bead sizes measured inside HeLa cells; as can be clearly observed the data are in very good agreement with both dynamic light scattering measurements (Figure S7) and *in vitro* STORM imaging (Figure S8), demonstrating the ability of STORM to accurately measure nanoparticle size inside cells. Not only can this average value be precisely determined, but the spread in size can also be assessed using these histograms. In this case, the

Gaussian distribution of individual NP sizes (solid lines in Figure 4C) implies the absence of particular subpopulations of NPs during internalization. To the best of our knowledge, this is the first example of accurate NP size distribution measurements inside cells by optical microscopy. Figure 4D shows averaged reconstructions for PS nanoparticles in HeLa cells, revealing the correct identification of size and morphology. This demonstrates that particle averaging, successfully used for protein complexes[24] and viral particles[31,32], is also an effective tool to investigate synthetic nanoparticles in cellular systems with even greater detail.

Having proven the potential of our methodology to accurately address individual nanoparticles inside cells, we focused on the study of a relevant biomedical challenge: the intracellular delivery of nanoparticulate antigens to antigen-presenting cells. This is of crucial importance to modulation the antigen-specific immune response towards cross-presentation and the induction of potent cellular immune response, and therefore is of great relevance with respect to development of novel vaccines[33]. Key steps in this process are the internalization of the nanoparticles by dendritic cells (DCs), their intracellular trafficking and the processing of the antigen[34]. Here we visualize the internalization of ovalbumin (OVA)-coated polystyrene nanoparticles by DCs. Note that OVA is a commonly used model antigen that is recognized by the murine immune studies and used a standard tool for *in vitro* and *in vivo* immuno-biological experiments. Figure 5A shows STORM images of OVA-loaded PS nanoparticles and their interactions with the plasma membrane.

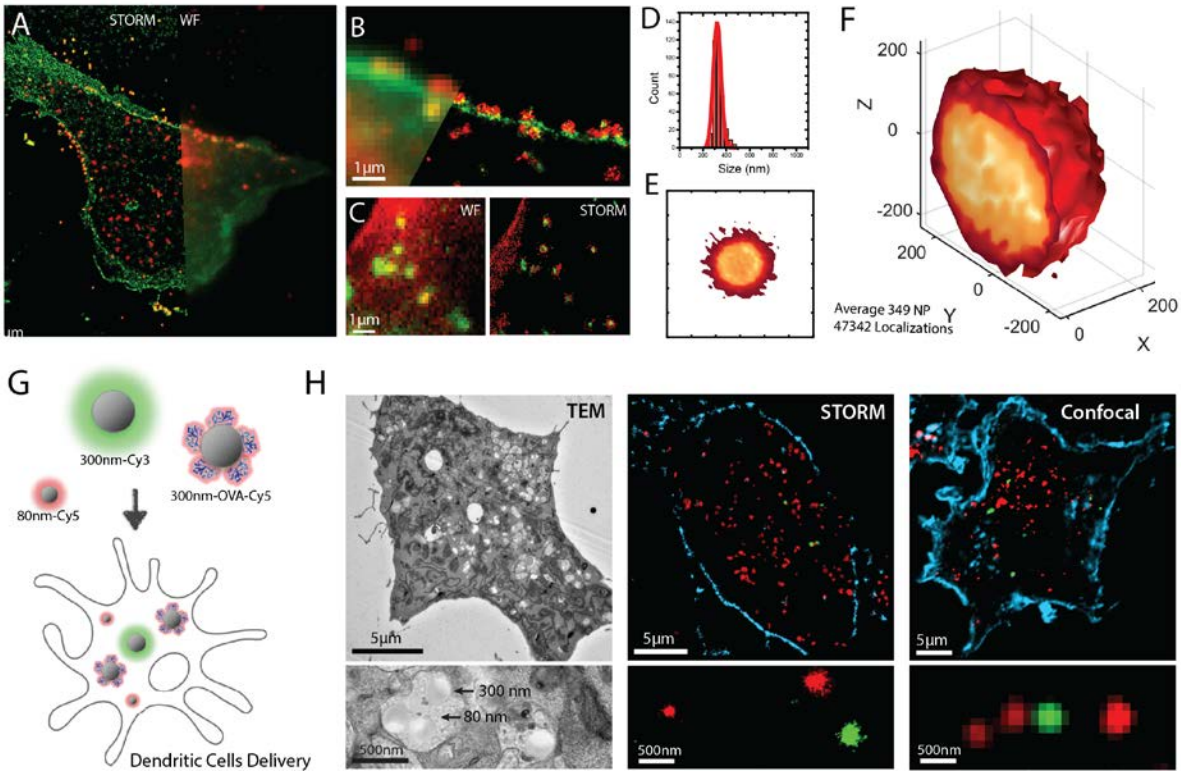

Figure 5 – STORM imaging of OVA-nanoparticle internalization by dendritic cells. A) Two-color imaging of membrane-stained DC (green) and OVA-NPs (red) in wide-field (right) and STORM (left). B) Magnification of the membrane highlighting individual nanoparticles bound to the plasma membrane and after internalization. C) Co-localization of OVA-NPs (cyan) with endosomal vesicles labeled by cholera toxin subunit B. D) Size histogram of internalized nanoparticles. E,F) Two- and three dimensional particle averaging of 250 nanoparticles over 20 different cells. G) Schematic representation of the experiment used to compare TEM, STORM and confocal microscopy. Three different nanoparticles (varying in size and color) are administered to DCs prior to fixation and imaging. H) TEM (left), STORM (middle) and confocal imaging (right) of the different nanoparticles inside DCs. Bottom panels are magnifications demonstrating the ability of the different techniques to image NPs of varying size and color.

In DCs, we were also able to resolve individual NPs and track them during membrane binding and internalization, as shown in the magnified image in Figure 5B. To gain more detailed information on NP internalization we labeled the plasma membrane and endocytic vesicles with alexa647-labeled cholera B toxin as shown in Figure 5C. The high resolution of STORM allows us to identify vesicle membrane contour and to identify individual nanoparticles in individual intracellular vesicles. We used the analysis tools described above to obtain

quantitative information about the nanoparticles inside DCs. The histogram in Figure 5D shows nanoparticle size distribution after internalization, and the measured size matches perfectly with the size of these nanoparticles measured by DLS (see Figure S7). Notably, here we labeled the antigen (OVA) rather than the nanoparticle itself, in order to track the active payload inside dendritic cells. Figures 5E and 5F show the 2D and 3D particle averaging of the OVA-beads within dendritic cells. The average size perfectly matches the administered nanoparticles, indicating that most of the payload is still loaded onto the NP and not yet processed[35]. Interestingly, the histogram of the number of localizations per NP (Figure S9) shows a broad distribution. As the number of localizations per bead is correlated with the number of antigens present[36], this may indicates partial processing of the OVA on the bead surface. We argue that the molecular counting ability of STORM can be used to evaluate the efficacy of antigen processing on different nanoparticles and provide rules for the design of novel and improved nanocarriers for intracellular antigen delivery.

We extensively discussed the potential of STORM for the study of nanoparticle entry and intracellular trafficking, comparing it wide-field microscopy. However, to fully appreciate the benefit STORM can offer for intracellular imaging of nanomedicines, we designed an experiment to be challenging for confocal and electron microscopy. DCs were incubated with a mixture of (i) 300 nm Alexa647-labeled OVA-coated NPs; (ii) 80 nm Alexa647-labeled carboxylic acid NPs and (iii) 300 nm Cy3-labeled amino beads, followed by STORM, confocal microscopy and TEM imaging as shown schematically in Figure 5G. The mixture of these three species represents a good benchmark to evaluate the ability of the different techniques to resolve differences in NP size and color. Figure 5H shows TEM, STORM and confocal images of NP-pulsed dendritic cells; in all the techniques it is possible to visualize particle internalization. However, whereas TEM does yield a high resolution, albeit with some issues for soft materials that have limited contrast upon uranyl acetate or osmium tetrachloride

staining (see also Figure S10), TEM does not yield any information on the nanoparticle color, and thus surface-functionalization. This is showcased in the lower panel of Figure 5H. The excellent resolution of TEM allows for discriminating between particles of different sizes, while at the same time solving the morphologies of the cellular structures in the surroundings, e.g. endosomal vesicles or plasma membrane. However, particles of the same size but different chemical functionality are not distinguishable. On the contrary, both confocal and STORM can differentiate between particles with different labeling. However, confocal microscopy is unable to discriminate between 300 nm and 80 nm particles as they fall below diffraction limit. Importantly STORM microscopy succeeds in distinguishing both particles varying in size and surface functionality, although not at the same resolution of TEM. Notably, confocal and STORM microscopy can be applied to live cell samples, a great advantage in the study of dynamic phenomena involving nanoparticles in living cells. In this regard, the development of live cell STORM for nanoparticles will represent a significant advance towards the understanding of nanoparticles trafficking in cells. Overall, STORM can fill the gap between electron and confocal microscopy and the development of correlative techniques able to superimpose STORM and TEM images can be of further use to the nanomedicine field[37].

Conclusion

In conclusion, the combination of STORM and single molecule analysis methods proposed here allows for quantitative investigation of nanoparticle interactions with the cell membrane and subsequent intracellular trafficking. The ability to directly visualize individual nanoparticles with nanometric resolution yields crucial information such as the mechanism of single endocytic events, intracellular particle size distribution and investigating the intracellular fate of a therapeutic payload. In this framework super resolution microscopy is an

ideal bridge between confocal and electron microscopy and represents a powerful tool towards the understanding of intracellular drug delivery.

Materials and Methods

Nanoparticles Labeling

Carboxylic acid functionalized polystyrene beads (Spherotech) were suspended at 0.25 %w/v in PBS (pH 7.2) followed by the addition of 10 eq. EDC, 25 eq. NHS and 0.6 eq. Alexa-647-Cadaverine (Invitrogen). Amine functionalized polystyrene beads (Spherotech) were suspended at 0.25 %w/v in bicarbonate buffer (pH 8.5) followed by the addition of 1 eq. Cy5-NHS. All reactions were shaken for 4h at room temperature. The beads were then centrifuged, the supernatant was removed, the beads were resuspended in water and extensively dialysed for 48h. 300 nm carboxylated PS nanoparticles (Spherotech) were functionalized with ovalbumin, Alexa Fluor 647 conjugate (OVA-AF647) according to the protocol provided by Life Technologies. NPs were analyzed by DLS and Zeta-potential measurements. NPs were diluted in water or PBS and measurements were conducted at 20˚C using Sarstedt UV Transparent Disposable Cuvettes (DLS) or Malvern Disposable Capillary Cells (Zeta) in a Malvern Instruments NanoZS ZEN3600 Zetasizer with a 632.8 nm Laser. Using the Malvern Zetasizer Software, an average result was obtained per bead type over three consecutive measurements of at least ten runs.

Cell Culture and staining

HeLa cells were plated in 8-wells LabTek Dishes (10.000 cells in 250 µL of medium) and cultured overnight at 37 °C and 5 % CO_2. Next, nanoparticle solution was added, followed by 4 h of culturing at 37 °C and 5 % CO_2. Cells were subsequently washed with PBS and fixed with 4% PFA for 10 minutes at room temperature. For colocalization studies the following markers were used: i) phalloidin-atto488 for actin staining, Wheat Germ Agglutinin (WGA)

alexa 568 for membrane and nuclear pore complex staining, 70KDa dextran alexa 568 for macropynosome staining. For membrane staining WGA-568 (1 µg/mL) was added for 5 minutes after cell fixation followed by PBS washing. For actin staining phalloin was used according to the provider recommendation. For macropynosome staining dextran (1mg/mL) was administered to HeLa for 30 min before washing with PBS and cell fixation. DC2.4 cells were plated on Willco-Dish glass bottom dishes (125.000 cells, suspended in 500 µL of culture medium) and cultured overnight at 37 °C and 5 % CO_2. Next, nanoparticle solution was added, followed by 24 h of culturing at 37 °C and 5 % CO_2. After fixation in 4 % paraformaldehyde, cells were stained with Hoechst (10 µL of a 1 mg/mL stock in DMSO) and CTB-AF488 (5 µL of a 1 mg/mL stock in PBS) for 40 min at room temperature.

STORM Imaging

Images were acquired using a Nikon N-STORM system configured for total internal reflection fluorescence (TIRF) imaging. Excitation inclination was tuned to adjust focus and to to maximize the signal-to-noise ratio. Fluorophores were excited illuminating the sample with the 647nm (~160 mW), 561 nm (~80 mW) and 488 nm (~80 mW) laser lines built into the microscope. Fluorescence was collected by means of a Nikon 100x, 1.4NA oil immersion objective and passed through a quad-band pass dichroic filter (97335 Nikon). Images were recorded onto a 256x256 pixel region (pixel size 170 nm) of a EMCCD camera (ixon3, Andor). Single molecules localization movies were analyzed with NIS element Nikon software. 3D measurements were performed using the astigmatism method. A prior calibration curve to relate the ellipticity of single fluorescent molecules to z-position was performed using fluorescent TetraSpeckTM microspheres 0.1 µm in diameter (Life-technologies, Molecular Probes®). Data was analyzed with NIS Elements (Nikon), ImageJ. The custom-made software for single molecule quantification is extensively described in the supplementary information.

Confocal Imaging

Confocal microscopy was carried out on a Leica DMI6000 B inverted microscope equipped with an oil immersion objective (Leica, 63x, NA 1.40) and attached to an Andor DSD2 confocal scanner. Images were processed with ImageJ software.

Transmission electron microscopy.

DC2.4 cells were plated in 24-well plates containing glass coverslips inside the wells (250 000 cells, suspended in 1 mL of culture medium) and cultured overnight at 37 °C and 5 % CO_2. Next, nanoparticle solution (*vide supra*) was added, followed by 24 h of culturing at 37 ° and 5 % CO_2. Culture medium was aspirated and cells were washed with PBS. Next, 1 mL of a fixing solution containing 4% paraformaldehyde and 2.5% glutaraldehyde in 0.1m Sodium cacodylate buffer (pH 7.2) was added and allowed to fixate for 4h at room temperature, followed by fixation overnight at 48 °C. After washing three times for 20 min with buffer solution, cells were dehydrated through a graded ethanol series, including a bulk staining with 1 % uranylacetate at the 50 % ethanol step followed by embedding in Spurr's resin. Ultrathin sections of a gold interference color were cut using an ultramicrotome (ultracut E/Reichert-Jung), followed by a post-staining with uranyl acetate and lead citrate in a Leica ultrastainer, and collected on formvar-coated copper slot grids. They were viewed with a transmission electron microscope 1010 (JEOL, Tokyo, Japan).

Acknowledgements

NVP and BGDG acknowledge BOF-UGhent and the FWO Flanders for funding. L.A is grateful for financial support from the Netherlands Organization for Scientific Research (NWO – VENI Grant: 722.014.010).

Competing Financial Interests

The authors declare no competing financial interests.

Supporting Information

The Supporting Information is available free of charge on the ACS Publications website.

- Single Molecule Data Analysis Software description. Figure S1 and S4 Confocal imaging of internalized nanoparticles. Figure S2 and S3 3D reconstruction of internalized nanoparticles. Figure S5 and S6 STORM colocalization. Figure S7 DLS of nanoparticles. Figure S8 in vitro STORM of NPs. Figure S9 histogram of NP localizations. Figure S10 TEM of internalized particles.

References

(1) Farokhzad, O. C.; Langer, R. Impact of Nanotechnology on Drug Delivery ACS Nano 2009, 3 (1), 16–20.

(2) Anselmo, A. C.; Mitragotri, S. An Overview of Clinical and Commercial Impact of Drug Delivery Systems J. Controlled Release 2014, 190, 15–28.

(3) Wright, J. Nanotechnology: Deliver on a Promise Nature 2014, 509 (7502), S58–S59.

(4) Nie, S. Understanding and Overcoming Major Barriers in Cancer Nanomedicine Nanomedicine 2010, 5 (4), 523–528.

(5) Torrano, A. A.; Blechinger, J.; Osseforth, C.; Argyo, C.; Reller, A.; Bein, T.; Michaelis, J.; Bräuchle, C. A Fast Analysis Method to Quantify Nanoparticle Uptake on a Single Cell Level Nanomedicine 2013, 8 (11), 1815–1828.

(6) Mühlfeld, C.; Rothen-Rutishauser, B.; Vanhecke, D.; Blank, F.; Gehr, P.; Ochs, M. Visualization and Quantitative Analysis of Nanoparticles in the Respiratory Tract by Transmission Electron Microscopy Part. Fibre. Toxicol. 2007, 4, 11.

(7) Möckl, L.; Lamb, D. C.; Bräuchle, C. Super-Resolved Fluorescence Microscopy: Nobel Prize in Chemistry 2014 for Eric Betzig, Stefan Hell, and William E. Moerner Angew. Chem., Int. Ed. Engl. 2014, 53 (51), 13972–13977.

(8) Hell, S. W. Nanoscopy with Focused Light (Nobel Lecture) Angew. Chem., Int. Ed. 2015, 54 (28), 8054–8066

(9) Kamiyama, D.; Huang, B. Development in the STORM Dev. Cell 2012, 23 (6), 1103–1110.

(10) Betzig, E. Single Molecules, Cells, and Super-Resolution Optics (Nobel Lecture) Angew. Chem., Int. Ed. 2015, 54 (28), 8034–8053.

(11) Gustafsson, M. G. L. Nonlinear Structured-Illumination Microscopy: Wide-Field Fluorescence Imaging with Theoretically Unlimited Resolution Proc. Natl. Acad. Sci. U. S. A. 2005, 102 (37), 13081–13086.

(12) Park, H.; Hoang, D. T.; Paeng, K.; Kaufman, L. J. Localizing Exciton Recombination Sites in Conformationally Distinct Single Conjugated Polymers by Super-Resolution Fluorescence Imaging ACS Nano 2015, 9 (3), 3151–3158.

(13) Albertazzi, L.; van der Zwaag, D.; Leenders, C. M. A.; Fitzner, R.; van der Hofstad, R. W.; Meijer, E. W. Probing Exchange Pathways in One-Dimensional Aggregates with Super-Resolution Microscopy Science 2014, 344 (6183), 491–495.

(14) Iinuma, R.; Ke, Y.; Jungmann, R.; Schlichthaerle, T.; Woehrstein, J. B.; Yin, P. Polyhedra Self-Assembled from DNA Tripods and Characterized with 3D DNA-PAINT Science 2014, 344 (6179), 65–69.

(15) Lee, S.-H.; Shin, J. Y.; Lee, A.; Bustamante, C. Counting Single Photoactivatable Fluorescent Molecules by Photoactivated Localization Microscopy (PALM) Proc. Natl. Acad. Sci. U. S. A. 2012, 109 (43), 17436–17441.

(16) Dempsey, G. T.; Vaughan, J. C.; Chen, K. H.; Bates, M.; Zhuang, X. Evaluation of Fluorophores for Optimal Performance in Localization-Based Super-Resolution Imaging Nat. Methods 2011, 8 (12), 1027–1036.

(17) Benke, A.; Olivier, N.; Gunzenhäuser, J.; Manley, S. Multicolor Single Molecule Tracking of Stochastically Active Synthetic Dyes Nano Lett. 2012, 12 (5), 2619–2624.

(18) Loos, C.; Syrovets, T.; Musyanovych, A.; Mailänder, V.; Landfester, K.; Nienhaus, G. U.; Simmet, T. Functionalized Polystyrene Nanoparticles as a Platform for Studying Bio–nano Interactions Beilstein J. Nanotechnol. 2014, 5, 2403–2412.

(19) Peters, B. P.; Ebisu, S.; Goldstein, I. J.; Flashner, M. Interaction of Wheat Germ Agglutinin with Sialic Acid Biochemistry (Moscow) 1979, 18 (24), 5505–5511.

(20) Huang, B.; Jones, S. A.; Brandenburg, B.; Zhuang, X. Whole-Cell 3D STORM Reveals Interactions between Cellular Structures with Nanometer-Scale Resolution Nat. Methods 2008, 5 (12), 1047–1052.

(21) Min, Y.; Caster, J. M.; Eblan, M. J.; Wang, A. Z. Clinical Translation of Nanomedicine Chem. Rev. 2015, 115 (19), 11147-11190.

(22) Albertazzi, L.; Fernandez-Villamarin, M.; Riguera, R.; Fernandez-Megia, E. Peripheral Functionalization of Dendrimers Regulates Internalization and Intracellular Trafficking in Living Cells Bioconjugate Chem. 2012, 23 (5), 1059–1068.

(23) Sahay, G.; Alakhova, D. Y.; Kabanov, A. V. Endocytosis of Nanomedicines J. Controlled Release 2010, 145 (3), 182–195.

(24) Albertazzi, L.; Serresi, M.; Albanese, A.; Beltram, F. Dendrimer Internalization and Intracellular Trafficking in Living Cells Mol. Pharmacol. 2010, 7 (3), 680–688.

(25) Carlini, L.; Manley, S. Live Intracellular Super-Resolution Imaging Using Site-Specific Stains ACS Chem. Biol. 2013, 8 (12), 2643–2648.

(26) Galbraith, C. G.; Galbraith, J. A. Super-Resolution Microscopy at a Glance J. Cell Sci. 2011, 124 (10), 1607–1611.

(27) Rossman, J. S.; Leser, G. P.; Lamb, R. A. Filamentous Influenza Virus Enters Cells via Macropinocytosis J. Virol. 2012, 86 (20), 10950–10960.

(28) Vandenberg, W.; Leutenegger, M.; Lasser, T.; Hofkens, J.; Dedecker, P. Diffraction-Unlimited Imaging: From Pretty Pictures to Hard Numbers Cell Tissue Res. 2015, 360 (1), 151–178.

(29) Szymborska, A.; Marco, A. de; Daigle, N.; Cordes, V. C.; Briggs, J. A. G.; Ellenberg, J. Nuclear Pore Scaffold Structure Analyzed by Super-Resolution Microscopy and Particle Averaging Science 2013, 341 (6146), 655–658.

(30) Broeken, J.; Johnson, H.; Lidke, D. S.; Liu, S.; Nieuwenhuizen, R. P. J.; Stallinga, S.; Lidke, K. A.; Rieger, B. Resolution Improvement by 3D Particle Averaging in Localization Microscopy Methods Appl. Fluoresc. 2015, 3 (1), 014003.

(31) Laine, R. F.; Albecka, A.; van de Linde, S.; Rees, E. J.; Crump, C. M.; Kaminski, C. F. Structural Analysis of Herpes Simplex Virus by Optical Super-Resolution Imaging. Nat. Commun. 2015, 6, 5980.

(32) Engelenburg, S. B. V.; Shtengel, G.; Sengupta, P.; Waki, K.; Jarnik, M.; Ablan, S. D.; Freed, E. O.; Hess, H. F.; Lippincott-Schwartz, J. Distribution of ESCRT Machinery at HIV Assembly Sites Reveals Virus Scaffolding of ESCRT Subunits Science 2014, 1247786.

(33) Irvine, D. J.; Hanson, M. C.; Rakhra, K.; Tokatlian, T. Synthetic Nanoparticles for Vaccines and Immunotherapy Chem. Rev. 2015, 115 (119), 11109-11146

(34) Cruz, L. J.; Tacken, P. J.; Zeelenberg, I. S.; Srinivas, M.; Bonetto, F.; Weigelin, B.; Eich, C.; de Vries, I. J.; Figdor, C. G. Tracking Targeted Bimodal Nanovaccines: Immune Responses and Routing in Cells, Tissue, and Whole Organism Mol. Pharmacol. 2014, 11 (12), 4299–4313.

(35) Houde, M.; Bertholet, S.; Gagnon, E.; Brunet, S.; Goyette, G.; Laplante, A.; Princiotta, M. F.; Thibault, P.; Sacks, D.; Desjardins, M. Phagosomes Are Competent Organelles for Antigen Cross-Presentation Nature 2003, 425 (6956), 402–406.

(36) Letschert, S.; Göhler, A.; Franke, C.; Bertleff-Zieschang, N.; Memmel, E.; Doose, S.; Seibel, J.; Sauer, M. Super-Resolution Imaging of Plasma Membrane Glycans Angew. Chem., Int. Ed. Engl. 2014, 53 (41), 10921–10924.

(37) Kim, D.; Deerinck, T. J.; Sigal, Y. M.; Babcock, H. P.; Ellisman, M. H.; Zhuang, X. Correlative Stochastic Optical Reconstruction Microscopy and Electron Microscopy PLoS One 2015, 10 (4), e0124581.